NANO LETTERS

pubs.acs.org/NanoLett

High Excitation Transfer Efficiency from Energy Relay Dyes in Dye-Sensitized Solar Cells

Brian E. Hardin,[†] Jun-Ho Yum,[‡] Eric T. Hoke,[§] Young Chul Jun,[§] Peter Péchy,[‡] Tomás Torres,[||] Mark L. Brongersma,[†] Md. Khaja Nazeeruddin,[‡] Michael Grätzel,[‡] and Michael D. McGehee*,[†]

[†]Department of Materials Science and Engineering, Stanford University, Stanford, California 94305, [‡]Laboratoire de Photonique et Interfaces, École Polytechnique Fédérale de Lausanne, CH-1015, Lausanne, Switzerland, [§]Department of Applied Physics, Stanford University, Stanford, California 94305, and [||]Departamento de Química Orgánica (C−I), Facultad de Ciencias, Universidad Autónoma de Madrid, Cantoblanco, 28049 Madrid, Spain

ABSTRACT The energy relay dye, 4-(Dicyanomethylene)-2-methyl-6-(4-dimethylaminostyryl)-4H-*pyran* (DCM), was used with a near-infrared sensitizing dye, TT1, to increase the overall power conversion efficiency of a dye-sensitized solar cell (DSC) from 3.5% to 4.5%. The unattached DCM dyes exhibit an average excitation transfer efficiency ($\bar{ETE}$) of 96% inside TT1-covered, mesostructured TiO_2 films. Further performance increases were limited by the solubility of DCM in an acetonitrile based electrolyte. This demonstration shows that energy relay dyes can be efficiently implemented in optimized dye-sensitized solar cells, but also highlights the need to design highly soluble energy relay dyes with high molar extinction coefficients.

KEYWORDS Solar cell, energy transfer, dye-sensitized dolar cell, energy relay dye, titania

Long range energy transfer has recently been used to increase light harvesting[1−7] inside of dye-sensitized solar cells (DSCs).[8−11] In one architecture, energy relay dyes (ERDs) absorb high-energy photons and transfer energy via Förster resonant energy transfer to the sensitizing dyes.[3−5,12] ERDs can both increase and broaden light absorption for the same film thickness in DSCs by increasing the overall dye loading. Because ERDs have a fundamentally different function and design rules than the sensitizing dyes, this architecture greatly expands the range of dyes that can be used in DSCs. In order for energy relay dyes (ERDs) to be used in state-of-the-art dye-sensitized solar cells, the excited ERDs must be able to efficiently transfer energy to the sensitizing dyes. Conventional DSCs are already efficient at absorbing visible light and collecting charges and can achieve external quantum efficiencies (EQE) of 85% at peak absorption.[13] The EQE contribution from the sensitizing dye is determined by the fraction of light absorbed by the sensitizing dye and the internal quantum efficiency (IQE). DSCs have high internal quantum efficiencies (>90%)[14−16] and in portions of the visible spectrum can absorb >90% of the light.

When photons are absorbed by the energy relay dye in ERD DSCs, they must undergo an additional energy transfer step before contributing to photocurrent; the EQE contribution from the relay dye (EQE_{ERD}) is thus defined by eq 1, where $\eta_{ABS,ERD}$ is the fraction of light absorbed by the ERD inside of the titania film and $\overline{ETE}$ is the average excitation transfer efficiency, or the average probability that an excited relay dye transfers its energy to a sensitizing dye. In order for ERDs to be viable in DSCs, excitation transfer efficiencies of over 90% are required to achieve a peak EQE of 85%.

$$EQE_{ERD} = \eta_{ABS,ERD} \cdot IQE \cdot \overline{ETE} \quad (1)$$

In our first report, only a minimum bound $\overline{ETE}$ of 46% could be estimated because of the uncertainty in determining $\eta_{ABS,ERD}$ due to light scattering caused by large TiO_2 nanoparticles and the inability to accurately measure the concentration of the dye because of rapid evaporation of the chloroform electrolyte during the electrolyte filling process.[4] In this report, the $\overline{ETE}$ is quantified by designing an experiment to accurately measure the light absorption by the energy relay dye inside of transparent TiO_2 electrodes and by developing a new ERD system that is more soluble in higher boiling point electrolyte solvents. A commercially available laser dye 4-(dicyanomethylene)-2-methyl-6-(4-dimethylaminostyryl)-4*H*-pyran (DCM)[17] was used as the ERD inside of the less volatile, conventional acetontitrile electrolyte to demonstrate an $\overline{ETE}$ of 96%. We also demonstrate increased performance in the optimized device architecture and find that the performance is limited by the relay dye's absorption and its moderate solubility in the electrolyte.

For near unity $\overline{ETE}$ to occur the rate of Förster resonant energy transfer (FRET) must be faster than radiative and nonradiative decay. The FRET rate is dependent on the separation distance between the ERD and sensitizing dye molecules and the Förster radius (R_0), which is the distance

* To whom correspondence should be addressed, mmcgehee@stanford.edu.
Received for review: 05/11/2010
Published on Web: 07/09/2010

DOI: 10.1021/nl1016688 | *Nano Lett.* **2010,** *10,* 3077–3083

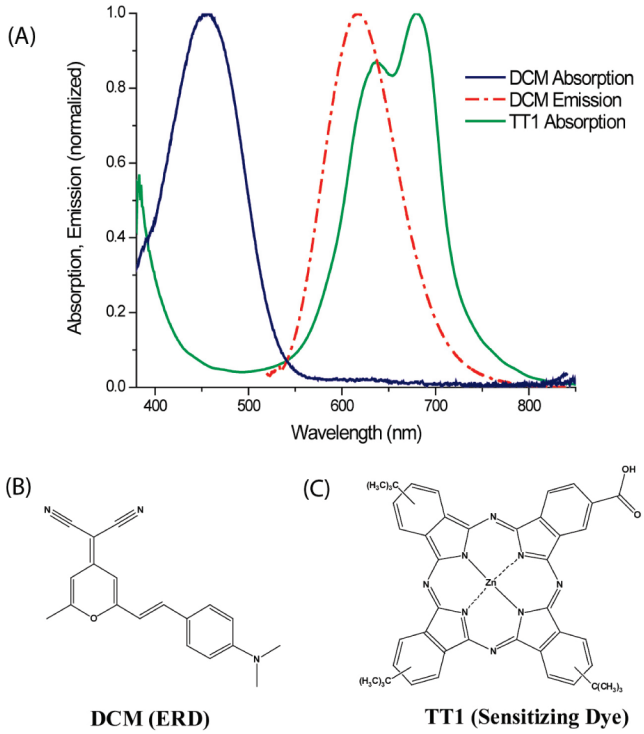

FIGURE 1. (A) Absorption (blue) and emission (red dash-dot) spectra of DCM energy relay dyes in acetonitrile:valeronitrile (85:15 vol) with TT1 absorption spectra on TiO_2 (green). Chemical structures of DCM (B) and TT1 (C).

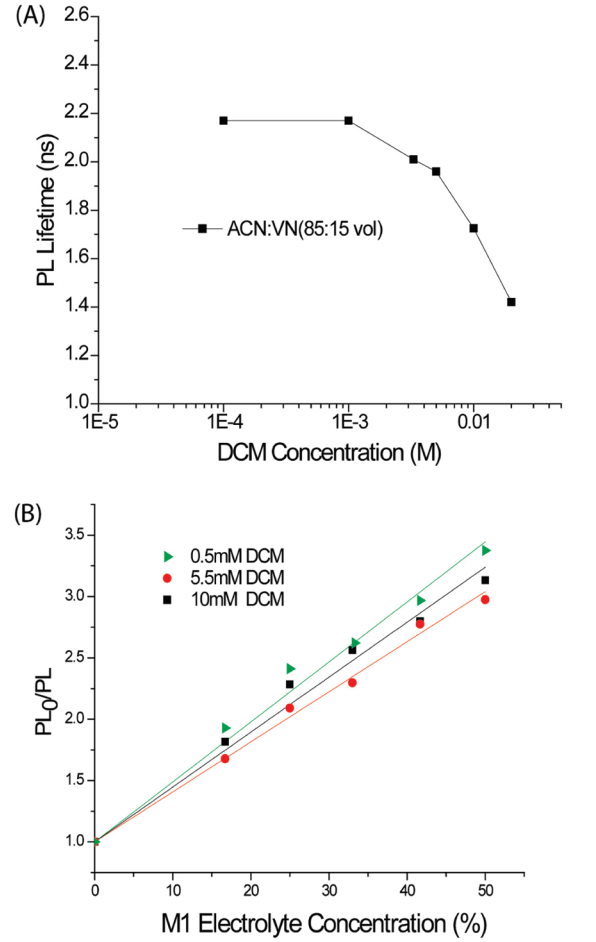

FIGURE 2. (A) Photoluminescence lifetime of DCM with various concentrations of ERD using an 85:15 mixture by volume of acetonitrile and valeronitrile. (B) Photoluminescence quenching caused by various concentrations of M1 electrolyte.

at which Förster energy transfer is 50% probable between individual chromophores and the photoluminescence (PL) lifetime.[18] The Förster radius typically ranges from 3 to 8 nm depending on the photoluminescence quantum efficiency of the ERD, the molar extinction coefficient of the sensitizing dye, and the overlap between ERD emission and sensitizing dye absorption spectra.

DCM is a strong ERD candidate because it has a broad absorption spectrum with a peak molar extinction coefficient of 44900 M^{-1} cm^{-1} at 460 nm, as shown in Figure 1a, a high photoluminescence quantum efficiency of 44% in acetonitrile,[19,20] and a short photoluminescence lifetime (~2 ns). The zinc phthalocyanine dye, TT1, was chosen as the sensitizing dye because it has an extremely high molar extinction coefficient with a peak of 191500 M^{-1} cm^{-1} centered at 680 nm.[4,21] The Föster radius from DCM to TT1 is 6.85 nm (eq S1, Supporting Information).

Quenching by the electrolyte and via ERD aggregation are two common nonradiative decay routes that directly impact the ETE. Figure 2A shows the photoluminescence lifetime of DCM versus DCM concentration for the common electrolyte mixture of acetonitrile/valeronitrile (85:15 vol). At relatively low DCM concentrations (10^{-4} to 10^{-3} M) the PL lifetime is constant. Increasing the DCM concentration above 1 mM reduces the PL lifetime from 2.1 to 1.2 ns, a 1.75× reduction in PL lifetime for the acetonitrile-based system. The DCM saturation limit, or the point when the concentration inside of the solution is not equivalent to the DCM mass divided by the solvent volume, is less than 18 mM in the acetonitrile/valeronitrile mixture. The PL lifetime reduction represents the dynamic quenching component caused by high dye loading; however, time-resolved PL spectroscopy does not account for static quenching (e.g., large aggregates that may be nonemissive).

Electrolyte quenching is mainly caused by the iodide/triiodide ions colliding with excited ERDs. TT1 devices are optimized using an electrolyte known as M1, which consists of 0.6 M 1-butyl-3-methylimidiazolium iodide (BMII), 0.025 M LiI, 0.05 M guanidinium thiocyanate, 0.28 M *tert*-butylpyridine, and 0.04 M I_2. Given the high concentrations, each ERD molecule collides with an ion more than once per nanosecond. Therefore FRET must occur at the subnanosecond time scale, which requires ERDs with short (<10 ns) photoluminescence lifetimes. DCM has a PL lifetime of 1.2−2.1 ns and has an electrolyte quenching rate between 4.0 and 4.9× compared to the natural decay rate depending on the DCM concentration as shown in Figure 2B (section S2 of Supporting Information). Combining the effects of both concentration and M1 electrolyte quenching produces an

DOI: 10.1021/nl1016688 | *Nano Lett.* **2010,** *10,* 3077–3083

overall dynamic quenching rate ($Q_{dynamic}$) of DCM between 4.88 (5 mM DCM with [M1] = 100%) and 8.00× (22 mM with [M1] = 100%) faster than natural decay rate (0.1 mM DCM with [M1] = 0%).

The nanopore size and surface concentration (C_A) of the sensitizing dye on TiO_2 are important because the overall transfer rate is equal to the sum of the individual FRET rates to each of the surrounding sensitizing dyes. Typical C_A values can range from 0.1 to 1 dye/nm^2 depending on the molecule size, number and type of attachment groups, TiO_2 particle size and crystal structure,[22,23] and the use of coadsorbents, which compete for TiO_2 adsorption sites but reduce dye aggregation. The sensitizing dye surface concentration was measured by desorbing TT1 from a titania film using 1 M KOH in pure ethanol and found to be $C_A = 0.389$ dye/nm^2 on the 17 nm diameter TiO_2 particles. The surface concentration is lower than that for standard dyes (e.g., N719), because a large concentration of chenodeoxychlic acid is required to coabsorb to the surface to reduce TT1 aggregation.[24]

We recently developed a model to determine how device and material parameters affect the $\overline{ETE}$.[12] Analogous to the Förster radius for individual chromophores is the critical radius (R_C), defined by eq 2. Pores which have a radius equal to the critical radius will have an $\overline{ETE}$ of ≥98% depending on the precise shape of the pore.

$$R_C = \left(\frac{C_A {R_0}^6}{1 + Q_{dynamic}} \right)^{1/4} \quad (2)$$

A large Förster radius, dense sensitizing dye surface concentration, and slow rate of dynamic quenching of the relay dye relative to its unquenched fluorescence decay rate ($Q_{dynamic}$) are all important for a large critical radius. It should be noted that the quenching rate only accounts for dynamic quenching, i.e. processes which shorten the excited state lifetime, and not static quenching, which occurs when a complex is formed between the dye and a quencher. In the model, nanopores were approximated as either cylinders or spheres and the concentration of the ERD inside of the nanopores was considered homogeneous.[12] Showa Denko 17 nm diameter titania nanoparticles were used in this study because they have the smallest average pore size, with an average pore diameter of 19.5 nm with a standard deviation of 5.4 nm (Figure S3, Supporting Information). Given the pore distribution in Figure S3, critical radii of 9 and 7 nm are required to achieve $\overline{ETE}$s above 90% assuming cylindrical and spherical pore geometries, respectively. The critical radius for the DCM/TT1 DSC is 8−9 nm depending on the quenching rate; given the pore size distribution of the 17 nm particles, the estimated $\overline{ETE}$ is 94% and 97% for cylindrical and spherical geometries, respectively (Figure S4, Supporting Information).

The $\overline{ETE}$ can be experimentally calculated from eq 1 by measuring the EQE contribution from the ERD (EQE_{ERD}), light absorption by ERD inside of the titania ($\eta_{abs,ERD}$), and the internal quantum efficiency of the system. Electrodes comprised of 5.4 μm thick titania films were fabricated using 17 nm TiO_2 nanoparticles. The 400 nm diameter titania particles that are often used in DSCs to scatter light were not employed so that the absorption could be more easily quantified. Films were dyed for 4 h in 1×10^{-4} M TT1 with 10 mM chenodeoxylic acid in ethanol. Various amounts of DCM were mixed into the M1 electrolyte. All other aspects of titania paste preparation and DSC fabrication and testing are the same as reported in literature.[4,25]

The IQE was determined by dividing the EQE at the peak wavelength of TT1, where the DCM does not absorb, by the fraction of light absorbed by TT1. UV−vis measurements indicate that <2% of the light is transmitted through the dyed TiO_2 films at 680 nm. An integrating sphere was used to determine that the reflection and absorption loss caused by the front contact (Hartford, Tech 15 glass) are approximately 10−13% at 680 nm (Figure S5, Supporting Information). For TT1-based DSCs shown in Figure 3a, the IQE ranged from 85 to 87%.

The EQE_{ERD} is determined by subtracting the EQE of ERD containing DSCs from the EQE of the control (0 mM DCM), as shown in Figure 3b. The change in EQE between 400 and 550 nm is attributed to the DCM photoresponse with a peak ΔEQE of 14.7%, 22.9%, and 28.2% for DCM concentrations of 5.5, 11, and 22 mM, respectively. The EQE_{ERD} does not appear to scale with the Beer−Lambert law given the DCM concentration, molar extinction coefficient, and film porosity (eq S6 in Supporting Information). Although dynamic quenching is expected to increase due to concentration quenching, a small increase in the dynamic quenching rate from 4.88× to 8.00× is not expected to appreciably change (<5%) the $\overline{ETE}$ and cannot account for the nonlinear improvement in EQE.[12] There is also a small (<5%) ΔEQE from 600 to 700, which is associated to slight differences in TT1 aggregation.[24] The observed increase in the EQE using transparent TiO_2 films is significant but not large enough to produce high efficiency devices due to insufficient absorption of light by the relay dye. For information on the current−voltage properties of the transparent DSCs see Table S7 in the Supporting Information.

In principle one can calculate the ERD absorption based on the ERD concentration in the prepared electrolyte and the titania film thickness and porosity (eq S6 Supporting Information). It is best, however, to measure $n_{abs,ERD}$ in case the concentration in the pores is not the same as that outside the titania film and because it is difficult to precisely determine the pore volume.[26,27] Direct measurement of $\eta_{abs,ERD}$ inside the pores is not possible because the Surlyn spacer is thicker than the TiO_2 film as shown in Figure 4a. The ERD containing electrolyte above the titania surface can absorb a significant fraction of the light. The $\eta_{abs,ERD}$ can be deter-

DOI: 10.1021/nl1016688 | Nano Lett. 2010, 10, 3077--3083

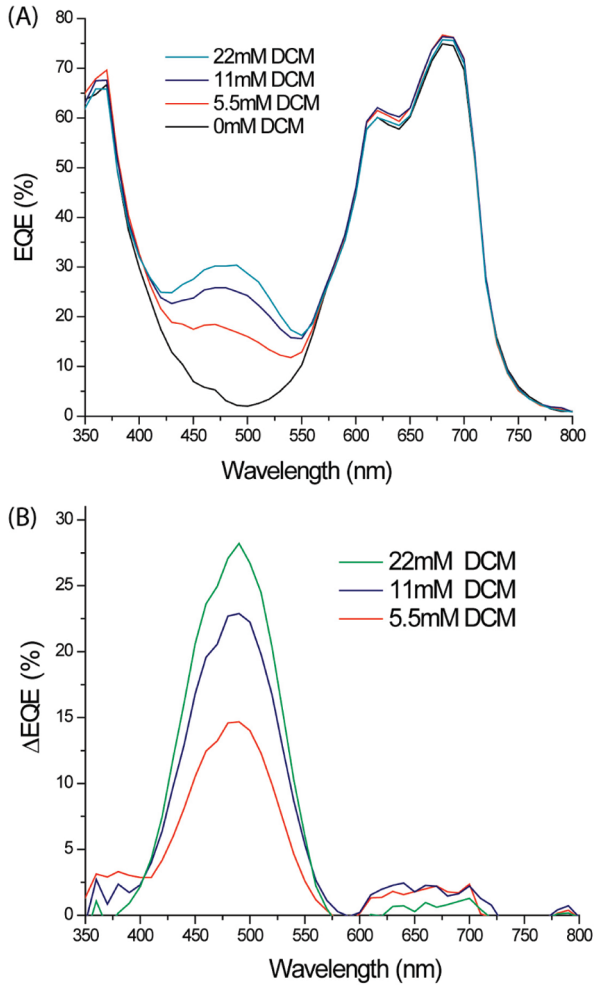

FIGURE 3. (A) External quantum efficiency of DSC of transparent TiO_2 electrodes (5.4 μm, 17 nm particles) with varying concentrations of DCM. (B) Change in the external quantum efficiency compared to control (0 mM) versus DCM concentration.

mined by comparing the differences between the optical density of the electrolyte filled region only (OD_{spacer}) versus the optical density of the TiO_2 region ($OD_{TiO_2+spacer}$); details are provided in section S8 in Supporting Information.

On the basis of this technique, the peak $\eta_{abs,ERD}$ was determined to be 16.7%, 27%, and 32−39% for 5.5, 11, and 22 mM DCM concentrations, as shown in Figure 4b. The deviation in $\eta_{abs,ERD}$ (represented by the error bars) is due to slight variation in film thickness within the samples (2−3%) and the variations in UV−vis measurements, which is <5% for low to moderate concentrations. At higher DCM concentrations (>18 mM), the standard deviation becomes greater due to the significant variation of the OD_{spacer} due to the sensitivity limit of the UV−vis detector with a small (1 × 1 mm) aperture. This technique can only be applied to systems with low overall ERD absorption; for devices with higher light absorption, this method cannot be used because the sensitivity limit of the UV−vis detector is reached.

As shown in Figure 4b, the ERD absorption scales with the EQE_{ERD}. Because the exact porosity is unknown, it is only possible to make qualitative statements about the DCM concentration inside of the pores versus DCM concentration in solution. At lower concentrations (i.e., 5.5 mM) the ERD concentration inside the nanopores (estimated 5.4 and 6.5 mM for an estimated porosity of 0.6 and 0.5, respectively) are equivalent or slightly higher than the ERD concentration in solution. The DCM molecule does not contain carboxylic or phosphonic acid groups typically used to attach to the TiO_2. However, DCM may physisorb to the TiO_2 due to electrostatic forces[28] or steric reasons[29] and thereby increase the dye loading inside of the film. At higher concentrations the estimated ERD absorption ($\eta_{abs,ERD} = 52\%$ for $c_{ERD} = 22$ mM, $p = 0.6$, $L = 5.4$ μm) is higher than the measured $\eta_{abs,ERD}$ of 32−39%. It is possible that the concentration of DCM inside of small pores is reduced due to aggregation. Dye solutions with more than 18 mM had noticeable precipitate formation at the bottom of the vial when allowed to settle for several hours. It is also possible that small aggregates exist in more dilute solutions which are not able to penetrate the mesoporous membranes that contain a small distribution of narrow (<10 nm) pores (see Figure S3, Supporting Information).

The $\overline{ETE}$ averaged over three DCM concentrations is 96% based on the EQE and $\eta_{abs,ERD}$ data from transparent films as shown in Figure 4C (Table S8, Supporting Information). The $\overline{ETE}$ values agree nicely with $\overline{ETE}$ modeling estimates of 94% and 97% for cylindrical and spherical pores, respectively. These high excitation transfer efficiency values compare well to DSC systems that covalently attach ERDs to TiO_2, which have obtained an $\overline{ETE}$ of >89%.[2]

It should be noted that alternative pathways exist for excited ERDs to contribute to photocurrent. Although DCM does not have anchoring groups to chemically attach to the titania, DCM can directly inject electrons into the TiO_2 when colliding with the titania surface. Control DSCs prepared with only chenodeoxychlic on the titania and 5.5 and 20 mM concentrations of DCM in the M1 electrolyte exhibit a peak EQE that is approximately 35% of the EQE_{ERD} for the DCM/TT1 system (Figure S9, Supporting Information). However, determining the exact contribution caused by direct injection to the $\overline{ETE}$ is challenging because the excited ERDs near the surface are highly likely to undergo FRET to a sensitizing dye before charge injection. For example, an excited DCM molecule separated by 1 nm from a TT1 acceptor will undergo FRET on the 20 fs time scale,[30] which is considerably faster than electron injection which occurs on the order of 100 ps for organic dyes such as TT1.[21] Therefore, although a portion of the EQE_{ERD} is likely caused by excited ERDs colliding on the surface in the DCM/TT1 system, it is unlikely that the $\overline{ETE}$ is artificially increased due to direct charge injection.

In an attempt to further improve the device performance, we placed DCM inside of an optimized TT1 device architecture, which contains an additional layer of light scattering titania nanoparticles. Conventional DSCs are typically com-

DOI: 10.1021/nl1016688 | *Nano Lett.* **2010,** *10,* 3077--3083

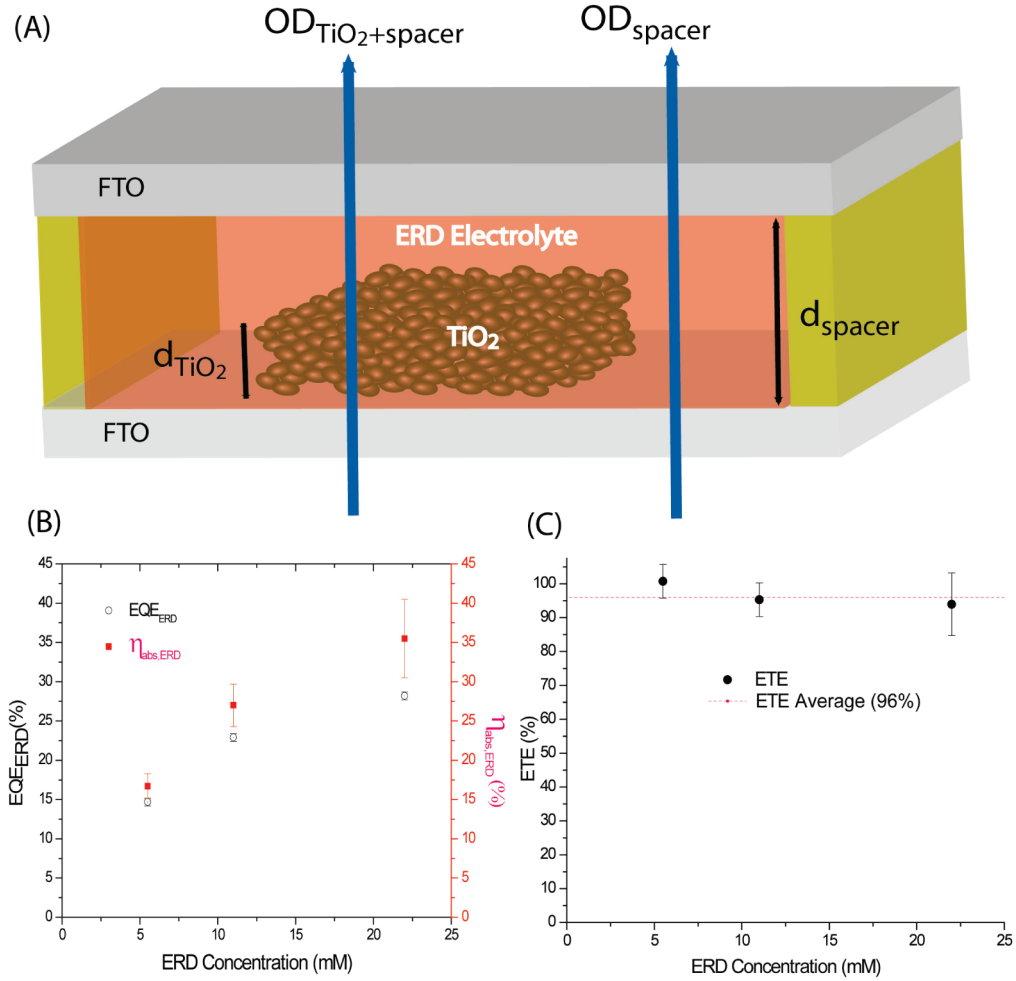

FIGURE 4. (A) Schematic of the ERD measurement to determine the amount of light absorbed by the ERD inside of the TiO_2 pores. (B) EQE_{ERD} (black circles) and $\eta_{abs,ERD}$ (red squares) versus predicted ERD concentration. (C) Average excitation transfer efficiency (ETE) versus concentration; the ETE average over three concentrations is 96%.

prised of 8 μm thick films made from either 17 or 25 nm diameter particles with a 4 μm thick layer of large (CCIC, HPW-400, 400 nm) TiO_2 particles.[31] The larger particles scatter light and in general have lower recombination rates, due to lower surface area, which allows for increased thickness and light absorption without large losses in the open-circuit voltage.[32]

The 8 + 4 μm device (8 μm of 17 nm particles with 4 μm of the scattering layer) was used with M1 electrolyte using a mixture of acetonitrile/valeronitrile (85:15 vol). The control device (0 mM) was 3.5% efficient at 1 sun with a short-circuit current density of 8.32 mA/cm^2, open-circuit voltage of 582 mV, and fill factor of 0.72. The control device is the most efficient TT1 DSC reported in literature with the electrode and M1 electrolyte considered optimal for the dye.[21] When 22 mM of DCM was placed inside of the M1 electrolyte, the device performance increased to 4.51%. The improvement is due to a 27% increase in the short circuit current density from the relay dye (10.61 mA/cm^2). The open-circuit voltage (590 mV) and fill factor (0.72) remained relatively unchanged. The EQE in the portion of the spectrum where DCM absorbs is 40%.

Using large nanoparticles did not improve light harvesting by the relay dye primarily because light scattering from 400-nm-particles occurs mainly in the red portion of the solar spectrum, where only the sensitizing dye absorbs. Furthermore, reducing the nanoparticle size (e.g., 200−250 nm TiO_2 particles) in the scattering layer to increase scattering where the energy relay dye absorbs is not expected to improve device performance. Light is largely scattered in the lateral and forward direction (i.e., light is diffracted forward rather than reflected backward), which means that light scattering occurs predominantly inside of the large nanoparticles.[33] It is believed that the pore sizes inside of the scattering layer are roughly on the order of the particle size. For efficient energy transfer, the ERDs must be within the R_C of the titania surface; consequently light absorbed by the ERDs inside the large pores has a low excitation transfer efficiency and hardly contributes to the photocurrent (Figure S4, Supporting Information).

DOI: 10.1021/nl1016688 | *Nano Lett.* **2010,** *10,* 3077–3083

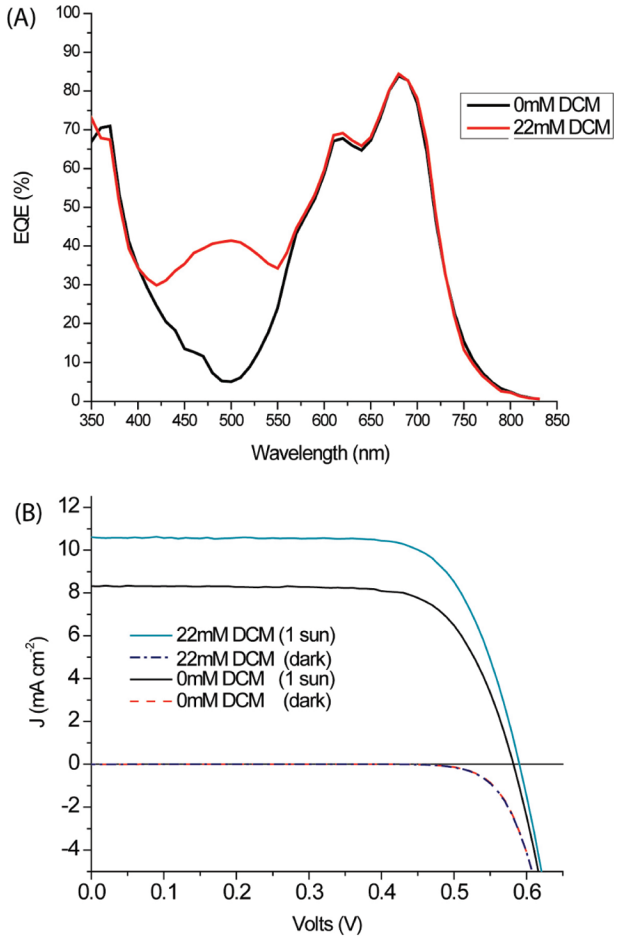

FIGURE 5. (A) The EQE of the 22 mM DCM DSC with 8 + 4 μm architecture using an acetonitrile-based electrolyte. (B) Photocurrent density−voltage (J−V) characteristics of devices with (22 mM DCM) and without (0 mM DCM) energy relay dye under AM 1.5G (100 mW/cm^2). Dashed lines represent the dark current for ERD containing and control devices.

An important question is whether a high $\overline{ETE}$ can be obtained for a variety of dyes in the DSC architecture. Many organic fluorophores have sufficiently fast PL lifetimes (<10 ns) to experience relatively low electrolyte quenching and PL quantum efficiencies greater than 25%, which may be sufficient when using highly absorbing organic sensitizing dyes with strong emission/absorption overlap for strong FRET.[34] Developing ERDs that provide >75% EQE_{ERD} will require a significant increase either in the molar extinction coefficient or in the solubility of the ERDs without significant concentration quenching. It is also possible to place multiple energy relay dyes inside the electrolyte that are chemically different to increase dye loading and light absorption. Future efforts should focus on developing multiple energy relay dye systems that absorb most of the light inside of 8−10 μm thick films before photons reach the light scattering layer.

Using the model DCM/TT1 DSC system, we were able to demonstrate extremely high average excitation transfer efficiency of over 95% with transparent TiO_2 films but could not increase the EQE_{ERD} above 40% in the optimized device architecture due to low ERD absorption. This work clearly shows that FRET from energy relay dyes to sensitizing dyes can be efficient enough for ERDs to be incorporated into state-of-the-art DSC systems. However, there are several important areas that should be researched and developed to fully determine the future prospects of high efficiency ERD DSCs. Although there have been studies which measure how dyes diffuse in nanoporous films based on molecule size[35] and membrane type,[36,37] there is relatively little information on dye loading and homogeneity of the dye concentration inside of nanopores. These areas should be further explored to determine the feasibility of high dye loading inside of mesostructured TiO_2 films. Finally, narrowly absorbing near-infrared dyes should be developed that have high internal quantum efficiencies and large open-circuit voltages. Near-infrared sensitizing dyes with a peak absorption >750 nm have been recently investigated[38] and have significant potential to provide major efficiency breakthroughs.

Acknowledgment. B. E. Hardin would like to thank Pascal Comte for preparing the TiO_2 films and BET measurements. J.-H. Yum thanks Dr. Shaik M. Zakeeruddin for preparing the electrolytes. This work was primarily supported by the Office of Naval Research Contract No. N00014-08-1-1163. M. McGehee acknowledges support from the Center for Advanced Molecular Photovoltaics through a grant from King Abdullah University of Science and Technology, and T. Torres acknowledges support from ESF-SOHYD Program, COST Action D35, and the EU Project ROBUST DSC, FP7-Energy-2007-1-RTD, No. 212792, MEC, Spain (CTQ2008-00418/BQU, CONSOLIDER-INGENIO 2010 CDS 2007-00010, PLE2009-0070, PSE-120000-2009-008 FOTOMOL), and CAM (MADRISOLAR-2, S2009/PPQ/1533).

Supporting Information Available. The FRET calculations, electrolyte quenching theory and experiments, device modeling, device performance, and referenced figures. This material is available free of charge via the Internet at http://pubs.acs.org.

REFERENCES AND NOTES

(1) Siegers, C.; Würfel, U.; Zistler, M.; Gores, H.; Hohl-Ebinger, J.; Hinsch, A.; Haag, R. *ChemPhysChem* **2008**, *9* (5), 793–798.
(2) Siegers, C.; Hohl-Ebinger, J.; Zimmermann, B.; Würfel, U.; Mülhaupt, R.; Hinsch, A.; Haag, R. *ChemPhysChem* **2007**, *8* (10), 1548–1556.
(3) Hardin, B. E.; Hoke, E. T.; Peters, C.; Geiger, T.; Nuesch, F.; Grätzel, M.; Nazeeruddin, M. K.; McGehee, M. D. In Long Range Forster Energy Transfer to Increase Light Absorption in Dye-Sensitized Solar Cells *Materials Research Society Fall Meeting, Boston, MA*; Materials Research Society: Boston, MA, 2008.
(4) Hardin, B. E.; Hoke, E. T.; Armstrong, P. B.; Yum, J.-H.; Comte, P.; Torres, T.; Frechet, J. M. J.; Nazeeruddin, M. K.; Grätzel, M.; McGehee, M. D. *Nat. Photonics* **2009**, *3* (7), 406–411.
(5) Yum, J. H.; Hardin, B. E.; Moon, S. J.; Baranoff, E.; Nüesch, F.; McGehee, M. D.; Grätzel, M.; Nazeeruddin, M. K. *Angew. Chem., Int. Ed.* **2009**, *48* (49), 9277–9280.
(6) Shankar, K.; Feng, X.; Grimes, C. A. *ACS Nano* **2009**, *3* (4), 788–794.
(7) Buhbut, S.; Itzhakov, S.; Tauber, E.; Shalom, M.; Hod, I.; Geiger, T.; Garini, Y.; Oron, D.; Zaban, A. *ACS Nano* **2010**.
(8) O'Regan, B.; Grätzel, M. *Nature* **1991**, *353*, 737–40.

DOI: 10.1021/nl1016688 | *Nano Lett.* **2010,** *10,* 3077–3083

(9) Hagfeldt, A.; Grätzel, M. *Acc. Chem. Res.* **2000**, *33* (5), 269–277.
(10) Snaith, H. J.; Schmidt-Mende, L. *Adv. Mater.* **2007**, *19* (20), 3187–3200.
(11) Peter, L. M. *Phys. Chem. Chem. Phys.* **2007**, *9*, 2630–2642.
(12) Hoke, E. T.; Hardin, B. E.; McGehee, M. D. *Opt. Express* **2010**, *18* (4), 3893–3904.
(13) Nazeeruddin, M. K.; De Angelis, F.; Fantacci, S.; Selloni, A.; Viscardi, G.; Liska, P.; Ito, S.; Takeru, B.; Grätzel, M. *J. Am. Chem. Soc.* **2005**, *127* (48), 16835–16847.
(14) Grätzel, M. *Inorg. Chem.* **2005**, *44* (20), 6841–6851.
(15) Barnes, P. R. F.; Liu, L.; Li, X.; Anderson, A. Y.; Kisserwan, H.; Ghaddar, T. H.; Durrant, J. R.; O'Regan, B. C. *Nano Lett.* **2009**, *9* (10), 3532–3538.
(16) Barnes, P. R. F.; Anderson, A. Y.; Koops, S. E.; Durrant, J. R.; O'Regan, B. C. *J. Phys. Chem. C* **2008**, *113* (3), 1126–1136.
(17) Hammond, P. R. *Opt. Commun.* **1979**, *29* (3), 331–333.
(18) Förster, T. *Discuss. Faraday Soc.* **1959**, *27*, 7.
(19) Bourson, J.; Valeur, B. *J. Phys. Chem.* **2002**, *93* (9), 3871–3876.
(20) Drake, J. M.; Lesiecki, M. L.; Camaioni, D. M. *Chem. Phys. Lett.* **1985**, *113* (6), 530–534.
(21) Cid, J.-J.; Yum, J.-H.; Jang, S.-R.; Nazeeruddin; Mohammad, K.; Martínez-Ferrero, E.; Palomares, E.; Ko, J.; Grätzel, M.; Torres, T. *Angew. Chem.* **2007**, *119* (44), 8510–8514.
(22) Lu, Y.; Choi, D.-J.; Nelson, J.; Yang, O. B.; Parkinson, B. A. *J. Electrochem. Soc.* **2006**, *153* (8), E131–E137.
(23) Ushiroda, S.; Ruzycki, N.; Lu, Y.; Spitler, M. T.; Parkinson, B. A. *J. Am. Chem. Soc.* **2005**, *127* (14), 5158–5168.
(24) Yum, J.-H.; Jang, S.-R.; Humphry-Baker, R.; Grätzel, M.; Cid, J.-J.; Torres, T.; Nazeeruddin, M. K. *Langmuir* **2008**, *24* (10), 5636–5640.
(25) Ito, S.; Murakami, T. N.; Comte, P.; Liska, P.; Grätzel, C.; Nazeeruddin, M. K.; Grätzel, M. *Thin Solid Films* **2008**, *516* (14), 4613–4619.
(26) Papageorgiou, N.; Barbe, C.; Grätzel, M. *J. Phys. Chem. B* **1998**, *102* (21), 4156–4164.
(27) Sommeling, P. M.; O'Regan, B. C.; Haswell, R. R.; Smit, H. J. P.; Bakker, N. J.; Smits, J. J. T.; Kroon, J. M.; van Roosmalen, J. A. M. *J. Phys. Chem. B* **2006**, *110* (39), 19191–19197.
(28) Kievsky, Y. Y.; Carey, B.; Naik, S.; Mangan, N.; ben-Avraham, D.; Sokolov, I. *J. Chem. Phys.* **2008**, *128* (15), 151102–5.
(29) Renkin, E. M. *J. Gen. Physiol.* **1953**, *38* (2), 225.
(30) FRET rate $= k_0(R_0/r)^6 = (1/2\ \text{ns})(6.85/1)^6 = 1/20$ fs.
(31) Wang, Z.-S.; Kawauchi, H.; Kashima, T.; Arakawa, H. *Coord. Chem. Rev.* **2004**, *248* (13−14), 1381–1389.
(32) Zhang, Z.; Ito, S.; O'Regan, B.; Kuang, D.; Zakeeruddin, S. M.; Liska, P.; Charvet, R.; Comte, P.; Nazeeruddin, M. K.; Pechy, P.; Humphry-Baker, R.; Koyangi, T.; Mizuno, T.; Grätzel, M. *Z. Phys. Chem.* **2007**, *221*, 319–327.
(33) Rothenberger, G.; Comte, P.; Grätzel, M. *Sol. Energy Mater. Sol. Cells* **1999**, *58* (3), 321–336.
(34) Lakowicz, J. R. *Principles of Fluorescence Spectroscopy*, *2nd* ed.; Plenum: New York, 1999.
(35) Hellriegel, C.; Kirstein, J.; Bräuchle, C. *New J. Phys.* **2005**, *7*, 23–23.
(36) Zurner, A.; Kirstein, J.; Doblinger, M.; Bräuchle, C.; Bein, T. *Nature* **2007**, *450* (7170), 705–708.
(37) Jung, C.; Hellriegel, C.; Michaelis, J.; Bräuchle, C. *Adv. Mater.* **2007**, *19* (7), 956–960.
(38) Macor, L.; Fungo, F.; Tempesti, T.; Durantini, E. N.; Otero, L.; Barea, E. M.; Fabregat-Santiago, F.; Bisquert, J. *Energy Environ. Sci.* **2009**, *2*, 529–534.

DOI: 10.1021/nl1016688 | *Nano Lett.* **2010,** *10,* 3077–-3083